Turbulent Fluid Dynamics
MAE 6233
Spring 2020

Blind Deconvolution of Turbulent Flows using Super-Resolution Reconstruction

Harsha Vaddireddy

School of Mechanical and Aerospace Engineering
Oklahoma State University

05/10/2020

Nomenclature

ω	DNS/high resolution Vorticity
ω^*	Reconstructed high resolution Vorticity
$\bar{\omega}$	Low/LES resolution Vorticity
$\bar{\psi}$	Low/LES resolution Streamfunction
ψ	DNS/high resolutionStreamfunction
ψ^*	Reconstructed high resolution Streamfunction
Re	Reynolds number
D	Discriminator
G	Generator
I	Reconstructed data
t	Time
x, y	Orthogonal spatial coordinates

Abstract

Turbulence is a complex flow phenomenon characterized by chaotic multiscale interactions which can be accurately modeled using direct numerical simulations (DNS). However, DNS is computationally prohibitive in many cases due to the fine grid requirement to resolve the high frequency content of the flow. Large eddy simulation (LES) attempts to relax this computational burden by resolving only large scales and modeling small scale interactions which is termed as the subgrid scale (SGS) modeling. One of the approaches to SGS modeling is approximate deconvolution (AD) procedure. In this work, we propose to use a machine learning algorithm called generative adversarial networks (GAN) to determine the deconvolved flow field instead of using traditional inverse filtering operation of AD. GANs have been demonstrated for image super-resolution by up sampling low resolution images. We use the enhanced super-resolution GAN (ESRGAN) framework for upscaling physical turbulence fields i.e, low-resolution LES field to super-resolution (close to DNS) field. The resulting super-resolved field can then be utilized to compute the SGS closure model instead of solving AD procedure numerically. In this work, ESRGAN framework is tested to super resolve two-dimensional decaying homogeneous turbulence flow field with physics bases constraints. The reconstruction of turbulent small scales by the proposed framework is evaluated by comparing to energy spectra on both super resolved and DNS field.

1 Introduction

Recent advances in machine learning approaches exceptionally deep learning have gained wide spread use and impact in many research communities. With advances in GPU to train these large datasets resulted in tremendous computational efficiencies in network training and the availability of rich historical labelled data have paved the huge success of deep learning in industrial solutions. An artificial neural network (ANN), also referred to as deep learning if multiple hidden layers are used, is a machine learning technique that transforms input features through nonlinear interactions and maps to output target features[1, 2]. ANNs attracted attention in recent times due to their exemplary performance in modelling complex nonlinear interactions across a wide range of applications including image processing[3], video classification[4] and autonomous driving [5].

Deep neural networks (DNN) have gained popularity in recent times due to their superior performance in modeling complex nonlinear interactions occurring in fluid dynamic problems. Tracey et al. [6, 7] used feed forward neural networks to target the source term($\hat{\nu}$) in SA model which is popular one equation closure model. The author's idea was to use results from using SA turbulence model(truth) and train neural networks on this data set to fit machine learning turbulence model to actual SA model accurately. These neural networks were shown capable of modeling the source term, synthesizing the concept of potential use of neural networks for turbulence modeling. Parish and Duraisway [8] proposed reconstructing modeling terms using Gaussian process inferred through Bayesian inversion. The use of Gaussian process is found to be not scalable especially for large CFD data sets. Zang and Duraiswamy [9] used neural networks to predict a correction factor for the turbulence production term in SA model. Ling et al. [10] used deep neural networks to learn Reynolds stress anisotropy tensor from high fidelity(DNS/LES) data. A key contribution of this seminal work is to train multi layer perceptron which embeds Galilean invariance into the predicted anisotropy tensor which makes the network architecture a true physics informed machine learning technique.

Recently convolutional neural networks (CNNs) have gained traction in fluid mechanics community. Tompson et al [11] and Xiao et al., [12] pioneered the usage of CNNs to solve Poisson equation. They have used CNN based models for simulating motion of smoke plumes around object. While the former used L2 based minimization, later used linear combination of L2 and divergence error to enforce physical constrains. These works primarily used to replace the Poisson solver which is the most computationally expensive part of Naiver-Stokes equation with CNNs to solve the Laplacian. Outside fluids community, Shan et al [13] investigated the application of CNNs to predict the electronic potential on cubic grids given the charge distribution with resulting speedups compared to traditional methods.

Advances in CNN lead to GAN networks which are used to generate new solutions of PDE-governed systems by training on existing datasets. Turbulent flow realizations generated from GANs are able to capture several statistical constraints of turbulent flows such as Komolgorov's $-5/3$ law and small scale intermittency of turbulence [14, 15]. Furthermore, to improve the performance and stability of GANs, temporal coherence were applied to GANs to generate super resolution realizations of turbulent flows [16]. Governing physical laws in the form stochastic differential equations were encoded into the architecture of GANs [17]. Inspired from dynamical systems, discriminator inputs were augments by using residuals and noise were introduce to training data [18]. Physical constraint such as conservation laws and statistical constraint derived from data distribution were embedded into the generator to improve the generalization capability of GANs based physical system emulator [19]. Realistic inflow boundary conditions for turbulent channel flow were produced by combining recurrent neural networks with GANs (RNN-GAN). The combination of RNN-GAN architecture could generate time-varying fully developed for a long time and were able to maintain spatio-temporal correlations for generated flow close to those of DNS [20]. Super Resolution GAN (SRGAN) and enhanced GAN (ESRGAN) were used to upscale 4^2 and 8^2 times for fluid flow problems such as flow over single and two cylinder with complicated wake flow [21]. These architectures were applied to upscale the PIV measurements which were limited to low spatial resolution [21].

Bode et al. [22] presented physics-informed ESRGAN (PIESRGAN) framework for subgrid scale modeling turbulent reactive flows. Their framework included loss function based on the the continuity equation to enforce the physics into the network. They illustrated the effective performance and extrapolation capability of PIESRGAN framework for decaying turbulence and LES of reactive spray in combustion process. Lee et al. [23] applied GANs for predicting the unsteady shedding of vortices behind a cylinder. They trained their GAN for two different Reynolds number and showed the capability of GAN to produce accurate results at interpolatory condition. In addition, they demonstrated the performance of GAN for predicting flow fields with larger time step interval compared the time step employed for training. Lee at al. [24] employed conditional GANs (cGANs) for predicting small eddies in three-dimensional turbulent mixing-layer. The cGANs are different from GANs in a way that it learns the mapping of input features and randomly generated noise to the output. Werhahn et al. [25] proposed the Multi-Pass GAN framework for super-resolution of three-dimensioal fluid flows. Their method decomposes generative problems on Cartesian field function into multiple smaller problems that can be learned effectively using two separate GANs. Specifically, first GAN upscales slices parallel to XY-plane and the second one refines the whole volume along Z-axis working on slices in the YZ-plane. This approach leads to shorter and robust training runs.

In this study we use physics constraint ESRGAN framework to learn the small scale turbulent features from low resolution turbulent field and thereby upscaling the field to high resolution field approximately to DNS fields. To this end, two dimensional decaying turbulence problem is chosen. The following describes the specific steps carried out for super resolution task.

1. Both DNS type resolution and LES type resolution of two dimensional decaying turbulence is simulated in vorticity stream function formulation.

2. The ESRGAN framework is developed with modified loss function containing physics based constraints to accurately predict the turbulent small structures (high wave number content).

3. The high resolution stream function (ψ) and vorticity (ω) fields are predicted from low resolution ($\bar{\psi}$) and ($\bar{\omega}$) using the trained generated network.

4. The energy spectrum $E(k)$ of super resolved field is compared with DNS along with bicubic and linear interpolatory schemes.

The details of 2D decaying turbulence numerical solver to generate DNS and LES data is described in Section 2. Furthermore, in same Section 2, we detail ESRGAN framework along with the loss function modification and associated hyperparameters. Section 3 describes the effectiveness of GANs for reconstruction and highlights limitations of the proposed framework. Furthermore, this section also lists the possible future work continuing this work. Finally, we will present the conclusions and summary in Section 4.

2 Materials and Methods

Computational Model

We specifically solve the system of PDEs called vorticity-streamfunction formulation. This system of PDEs contains the vorticity transport equation derived from taking the curl of the 2D incompressible Navier-Stokes equations and the Poisson equation representing the kinematic relationship between the streamfunction (ψ) and vorticity (ω). The resulting vorticity-streamfunction formulation is given as,

$$\left.\begin{aligned} \omega_t + J(\omega,\psi) &= \frac{1}{\text{Re}}\nabla^2\omega \\ \nabla^2\psi &= -\omega \end{aligned}\right\} \tag{1}$$

where the Reynolds number is set to Re $= 4000$. In Eq. 1, $J(\omega,\psi)$ is the Jacobian term given as $\psi_y\omega_x - \psi_x\omega_y$. The DNS vorticity field ω and streamfunction fieldψ are obtained by solving the Eq. 1 numerically. We use a third-order Runge-Kutta scheme for the time integration, and a second order Arakawa scheme [26] for the discretization of the Jacobian term $J(\omega,\psi)$. As we have a periodic domain, we use a fast Fourier transform (FFT) for solving the Poisson equation in Eq. 1 to obtain the streamfunction at every time step. We use a square domain of length 2π with periodic boundary conditions in both directions. We simulate homogeneous isotropic decaying turbulence which may be specified by an initial energy spectrum that decays through time. High fidelity DNS simulations are carried out for Re $= 4000$ with 256×256 resolution from time $t = 0$ to $t = 4.0$ with time step 0.001. The filtered flow quantities i.e., low resolution data ($\bar{\psi}$) and ($\bar{\omega}$) are obtained from coarsening the DNS quantities resulting in 32×32 resolution. The further details of solver and coarsening can be found in San and Staples[27].

Enhanced Super Resolution Framework (ESRGAN)

The framework of generative adversarial network (GAN) was first introduced by Goodfellow et al.[28]. In contrast to the structures of the traditional neural networks, the GAN consists of two "adversarial" networks, which are defined as a generator network G shown in Figure 2 and a discriminator network D shown in figure 3. The generator network Figure 2 generates fake images that are as similar as possible to the real images (ground truth), while the discriminator network is trained to distinguish the fake images from real images. Both G and D could be multilayer perceptrons and are trained simultaneously. In the most ideal conditions, after sufficient epochs of training, the generator network is essentially able to capture the real data distribution, while the "smart" discriminator network is unable to distinguish the generated images from the ground truth. This process is just like playing a two-player minimax game, which can be described with the following value function V(D, G):

$$min_G \ max_D \ V(D,G) = \mathbb{E}_{x\sim p_{data}(x)}[log(D(x)] + \mathbb{E}_{z\sim pz(z)}[log(1 - D(G(z)], \tag{2}$$

distribution possibility of the real images, and $D(I)$ represents the probability that I came from the real images rather than the generated images. $z$is the random noise of input generator network G, $G(z)$ is the generated fake image of G, and $D(G(z))$ is the probability of judging whether $G(z)$ came from the real images or not. During the whole training process, the generator network G wants to make the value of $D(G(z))$ as large as possible, which will decrease the value of $V(D,G)$. As for the discriminator network D, it tries to increase the $D(I)$ and decrease the $D(G(z))$, which will increase the $V(D,G)$. Therefore, the function $V(D,G)$ attempts to adjust the parameters of G to minimize $[log(1-D(G(z)))]$ and adjust the parameters of D to maximize $[logD(I)]$. Since the proposed framework combines discriminator and generator networks, the generative adversarial networks have resulted in benefits that have yielded a series of variant networks. Among them is the ESRGAN framework [29] specially designed for realizing the super-resolution reconstruction from low-resolution images. The ESRGAN network is shown in Figure 4. The loss function used in the minimizing the weights in GAN network is given below,

$$\mathcal{L} = \alpha \; l_{MSE} + \lambda \; l_{adv} + \beta \; l_{grad} + \gamma \; l_{continuity} + \delta \; l_{enstrophy}, \tag{3}$$

where $\alpha, \beta, \gamma, \lambda$ and δ are weighting coefficients for different loss term contribution. l_{MSE} is pixel wise mean squared error between DNS and reconstructed fields. l_{adv} is the discriminator/generator relativistic adversarial loss. l_{grad} is the pixel wise mean squared error between gradient of DNS and reconstructed fields which may help the generator network be more sensitive in generating high frequency content to close to DNS fields. $l_{continuity}$ and $l_{enstrophy}$ is the physics based constraint added to help the network in faster convergence and removing non physical solutions. The physics based constrain used in the current work is,

$$\begin{aligned} l_{cont} &= \nabla^2 \psi^* - \omega^* \\ l_{enstrophy} &= \omega^2 - \omega^{2*}, \end{aligned} \tag{4}$$

where ψ^* and ω^* are reconstructed high resolution fields. The values of coefficients are set to $\alpha = 5.0$,,$\beta = 0.1$, $\gamma = 0.01$, $\delta = 0.1$ and $\lambda = 1 \times 10^{-5}$. These are result of trail and error and different setting may result in similar and more accurate results. The total data set includes 400 time snapshots of low and high resolution vorticity and stream function flow fields. The training data consists of 300 time snapshots of low and high resolution data and testing the resulting GAN model on final 400^{th} time snapshot which corresponds to time $t = 4.0$s. The training is done by sending batch size of 32 random snapshots to conserve the memory constraints. The total training epochs are set to 20000 as after which there is no considerable change in reconstructed fields.

3 Results and Discussion

This study is mainly limited to *apriori* prediction of high resolution fields from low resolution data using ESRGAN framework. The low resolution (32^2) input is used to reconstruct high resolution (256^2) field which approximately equal to DNS field. Figure 5 shows the reconstructed stream function field. As we can observe GANs were able to interpolate and add the finer structure details to the low resolution stream function field. Similarly Figure 6 shows the reconstruction vorticity field. The reconstructed vorticity filed shows that GANs are able to add high frequency contents but not able to predict more smother field close to DNS. This is due to the addition of physics based constraints to the loss function. The MSE loss (l_{MSE}) is generally used for driving the optimization of network. Using this loss alone would predict smother fields but lacks the ability to add high frequency content to the low resolution field making it inefficient interpolation network. The addition of continuity and enstropy losses makes generator more accurate in predictions of high resolution filed and hence the non smooth filed but accurate in terms of adding high frequency content. The loss functions use finite difference based approximations for calculating derivatives required to calculate gradients. The truncation error associated with the numerical schemes may also be the reason for non smother fields. Figure 7 shows the energy spectrum $E(k)$ of DNS, reconstructed and FDNS along with traditional interpolate schemes. Both linear and bicubic interpolation results in more dissipative fields as they lack the prediction of high frequency content. ESRGAN predicts the spectrum statistics closer to the DNS field. This shows that GANs are not simple interpolatory models but rather try to learn the missing frequencies by referring to the output data.

Limitations

Machine learning (deep learning) models lack the generalization i.e., it predicts poorly outside the train data. The moment new physics is added to the testing data which is not incorporated in training data, these models collapse. Apart from this main limitation, deep learning models are black box in nature i.e., they are not open to interpret. This results in non physical solutions and stability issues in actual *aposteriori* deployment. Furthermore, large amount of data is required for deep learning based models to make accurate predictions. GANs specifically suffer from huge memory requirements as we increase the resolution or use 3D data. For larger resolution?dimensional data, the data should be split into multiple components for training which increases the complexity of data preprocessing. Practical CFD simulations are done on unstructured data which cannot be used straight forward for CNN/GAN based approaches due to its requirement of Cartesian meshes. One way around this is to use Jacobian transformation on unstructured grid to structured grid and train the GANs in the transformed space.

Recommendations for future work

The future work of this study includes,

- *Aposteriori* simulations using ESRGAN model as structure modelling technique rather than using traditional approximate deconvolutional (AD) technique. The following steps are required to achmeive this,
  1. Use the ESRGAN framework to reconstruct ω^* and ψ^* from low resolution filtered quantities $\bar{\omega}$ and $\bar{\psi}$ respectively.
  2. Use the ω^* and ψ^* in calculating the SGS closure term $\overline{J(\omega, \psi)}$.
  3. use the computed filtered $\bar{\omega}$ and $\bar{\psi}$ fields to advance to next time step.
- One more direction worth studying is to use GANs in solving the Poisson equation given in Eq. 1 and removing the traditional FFT solver which is most computationally intensive part in solving the Eq. 1. This will result in tremendous increase the computational speed up for cases that are within the training regime.

4 Conclusions

1. ESRGAN framework with modified loss functions containing physics based constraints is developed for super resolution of turbulent fields. The 2D decaying turbulence problem is selected for the purpose of easy demonstration.

2. *Apriori* analysis of turbulent field reconstruction show that ESRGANs are able to learn the high frequency content rather than just interpolating the data.

3. Physics based loss functions clearly helps in adding finer structure to the low resolution fields and there by accurately predicting the turbulent statistics closer to the DNS fields. This also resulted in non smoother flow field predictions which need further studies to generate more smoother fields.

References

[1] LeCun, Y., Bengio, Y., and Hinton, G., 2015. "Deep learning". *nature,* ***521***(7553), pp. 436–444.

[2] LeCun, Y., Bengio, Y., and Hinton, G., 2015. "Deep learning". *Nature,* ***521***(7553), p. 436.

[3] Ciregan, D., Meier, U., and Schmidhuber, J., 2012. "Multi-column deep neural networks for image classification". In 2012 IEEE Conference on Computer Vision and Pattern Recognition, pp. 3642–3649.

[4] Karpathy, A., and Fei-Fei, L., 2015. "Deep visual-semantic alignments for generating image descriptions". In Proceedings of the IEEE Conference on Computer Vision and Pattern Recognition, pp. 3128–3137.

[5] Sallab, A. E., Abdou, M., Perot, E., and Yogamani, S., 2017. "Deep reinforcement learning framework for autonomous driving". *Electronic Imaging,* ***2017***(19), pp. 70–76.

[6] Tracey, B. D., Duraisamy, K., and Alonso, J. J., 2015. "A machine learning strategy to assist turbulence model development". In 53rd AIAA aerospace sciences meeting, p. 1287.

[7] Tracey, B., Duraisamy, K., and Alonso, J., 2013. "Application of supervised learning to quantify uncertainties in turbulence and combustion modeling". In 51st AIAA Aerospace Sciences Meeting including the New Horizons Forum and Aerospace Exposition, p. 259.

[8] Parish, E. J., and Duraisamy, K., 2016. "A paradigm for data-driven predictive modeling using field inversion and machine learning". *Journal of Computational Physics,* ***305***, pp. 758–774.

[9] Zhang, Z. J., and Duraisamy, K., 2015. "Machine learning methods for data-driven turbulence modeling". In 22nd AIAA Computational Fluid Dynamics Conference, p. 2460.

[10] Ling, J., Kurzawski, A., and Templeton, J., 2016. "Reynolds averaged turbulence modelling using deep neural networks with embedded invariance". *Journal of Fluid Mechanics,* ***807***, pp. 155–166.

[11] Tompson, J., Schlachter, K., Sprechmann, P., and Perlin, K., 2017. "Accelerating eulerian fluid simulation with convolutional networks". In Proceedings of the 34th International Conference on Machine Learning-Volume 70, JMLR. org, pp. 3424–3433.

[12] Xiao, X., Zhou, Y., Wang, H., and Yang, X., 2018. "A novel cnn-based poisson solver for fluid simulation". *IEEE transactions on visualization and computer graphics.*

[13] Tang, W., Shan, T., Dang, X., Li, M., Yang, F., Xu, S., and Wu, J., 2017. "Study on a poisson's equation solver based on deep learning technique". In 2017 IEEE Electrical Design of Advanced Packaging and Systems Symposium (EDAPS), IEEE, pp. 1–3.

[14] King, R., Hennigh, O., Mohan, A., and Chertkov, M., 2018. "From deep to physics-informed learning of turbulence: Diagnostics". *arXiv preprint arXiv:1810.07785.*

[15] Chertkov, M., Hennigh, O., King, R., and Mohan, A., 2018. "From deep to physics-informed learning of turbulence: Diagnostics". *Bulletin of the American Physical Society,* ***63***.

[16] Xie, Y., Franz, E., Chu, M., and Thuerey, N., 2018. "tempogan: A temporally coherent, volumetric gan for super-resolution fluid flow". *ACM Transactions on Graphics (TOG),* ***37***(4), pp. 1–15.

[17] Yang, L., Zhang, D., and Karniadakis, G. E., 2018. "Physics-informed generative adversarial networks for stochastic differential equations". *arXiv preprint arXiv:1811.02033.*

[18] Stinis, P., Hagge, T., Tartakovsky, A. M., and Yeung, E., 2019. "Enforcing constraints for interpolation and extrapolation in generative adversarial networks". *Journal of Computational Physics,* ***397***, p. 108844.

[19] Wu, J.-L., Kashinath, K., Albert, A., Chirila, D., Xiao, H., et al., 2020. "Enforcing statistical constraints in generative adversarial networks for modeling chaotic dynamical systems". *Journal of Computational Physics,* ***406***, p. 109209.

[20] Kim, J., and Lee, C., 2020. "Deep unsupervised learning of turbulence for inflow generation at various reynolds numbers". *Journal of Computational Physics*, p. 109216.

[21] Deng, Z., He, C., Liu, Y., and Kim, K. C., 2019. "Super-resolution reconstruction of turbulent velocity fields using a generative adversarial network-based artificial intelligence framework". *Physics of Fluids,* ***31***(12), p. 125111.

[22] Bode, M., Gauding, M., Lian, Z., Denker, D., Davidovic, M., Kleinheinz, K., Jitsev, J., and Pitsch, H., 2019. "Using physics-informed super-resolution generative adversarial networks for subgrid modeling in turbulent reactive flows". *arXiv preprint arXiv:1911.11380.*

[23] Lee, S., and You, D., 2017. "Prediction of laminar vortex shedding over a cylinder using deep learning". *arXiv preprint arXiv:1712.07854.*

[24] Lee, J., Lee, S., and You, D., 2018. "Deep learning approach in multi-scale prediction of turbulent mixing-layer". *arXiv preprint arXiv:1809.07021.*

[25] Werhahn, M., Xie, Y., Chu, M., and Thuerey, N., 2019. "A multi-pass gan for fluid flow super-resolution". *Proceedings of the ACM on Computer Graphics and Interactive Techniques,* ***2***(2), pp. 1–21.

[26] Arakawa, A., 1966. "Computational design for long-term numerical integration of the equations of fluid motion: Two-dimensional incompressible flow. part i". *Journal of Computational Physics,* ***1***(1), pp. 119–143.

[27] San, O., and Staples, A. E., 2012. "High-order methods for decaying two-dimensional homogeneous isotropic turbulence". *Computers & Fluids,* ***63***, pp. 105–127.

[28] Goodfellow, I., Pouget-Abadie, J., Mirza, M., Xu, B., Warde-Farley, D., Ozair, S., Courville, A., and Bengio, Y., 2014. "Generative adversarial nets". In Advances in neural information processing systems, pp. 2672–2680.

[29] Wang, X., Yu, K., Wu, S., Gu, J., Liu, Y., Dong, C., Qiao, Y., and Change Loy, C., 2018. "Esrgan: Enhanced super-resolution generative adversarial networks". In Proceedings of the European Conference on Computer Vision (ECCV), pp. 0–0.

Figures

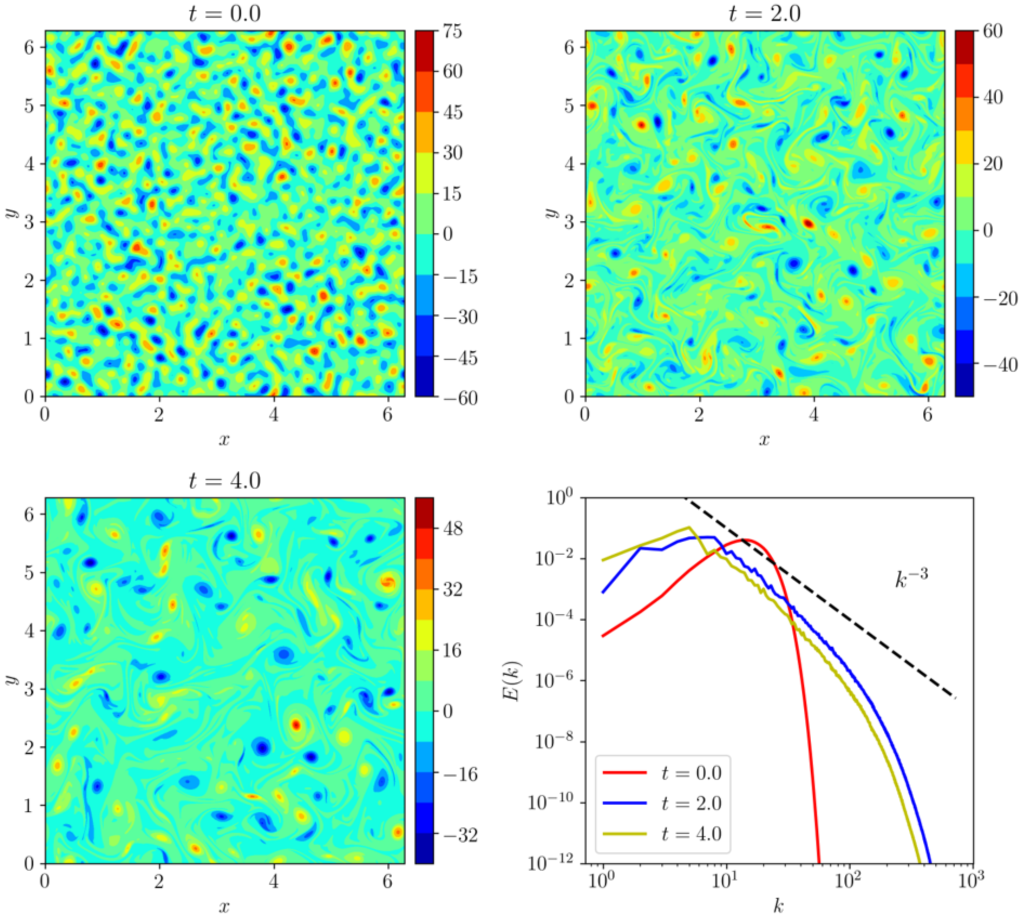

Figure 1: 2D decaying turbulence form time $t = 0.0$ to $t = 4.0$ for Re=4000 at grid resolution 256 × 256.

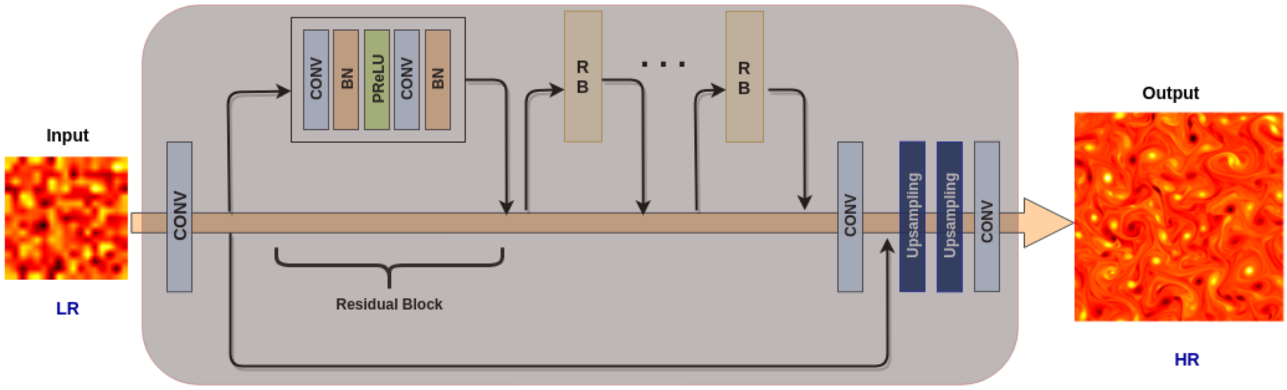

Figure 2: Convolutional generator network.

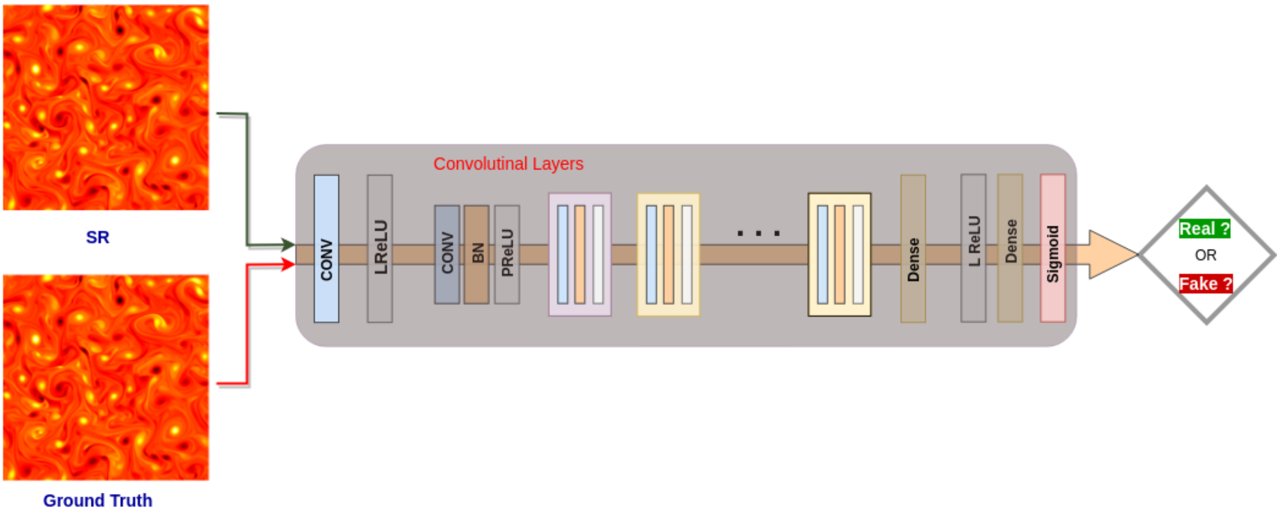

Figure 3: Convolutional discriminator network.

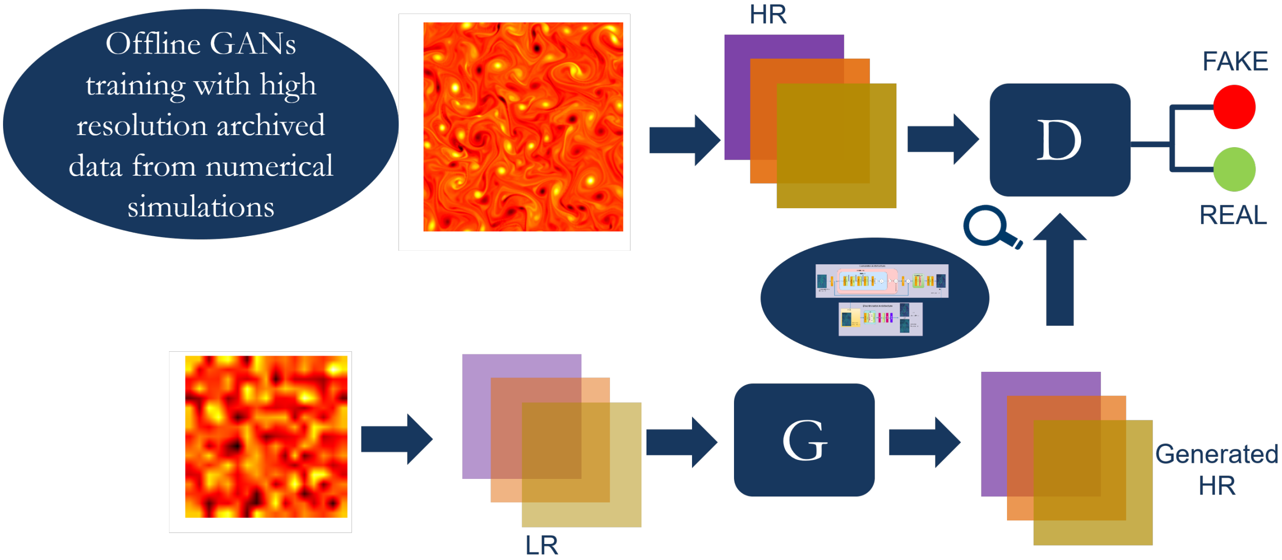
Offline GANs training with high resolution archived data from numerical simulations
HR
D
FAKE
REAL
G
LR
Generated HR

Figure 4: Enhanced super resolution generative adversarial network.

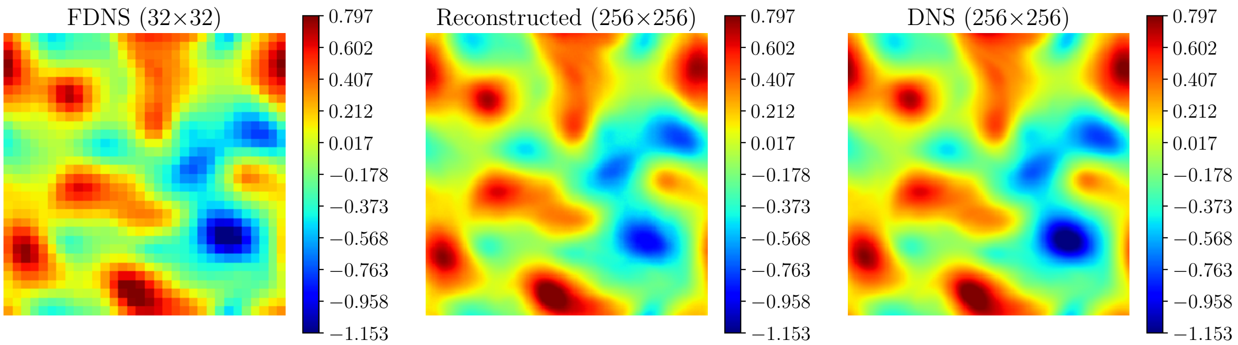

Figure 5: Reconstructed Stream function (ψ) at time $t = 4.0$ s. FDNS refers to filleted DNS field.

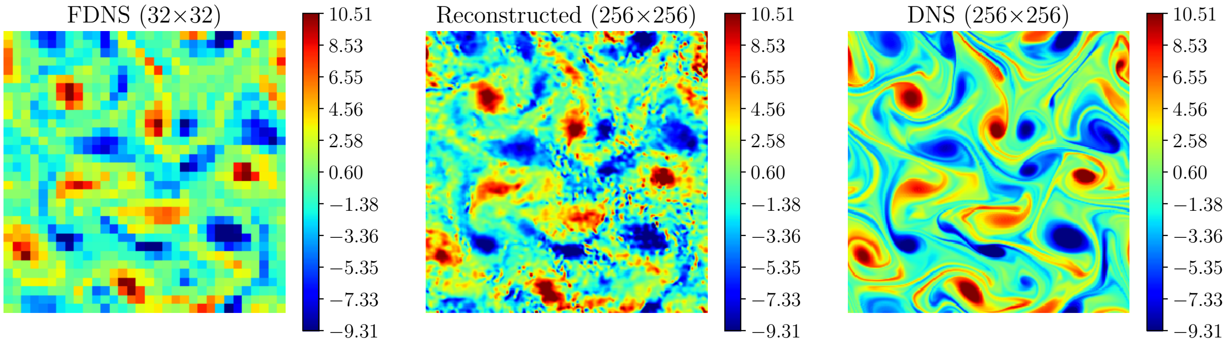

Figure 6: Reconstructed vorticity (ω) at time $t = 4.0$ s. FDNS refers to filleted DNS field.

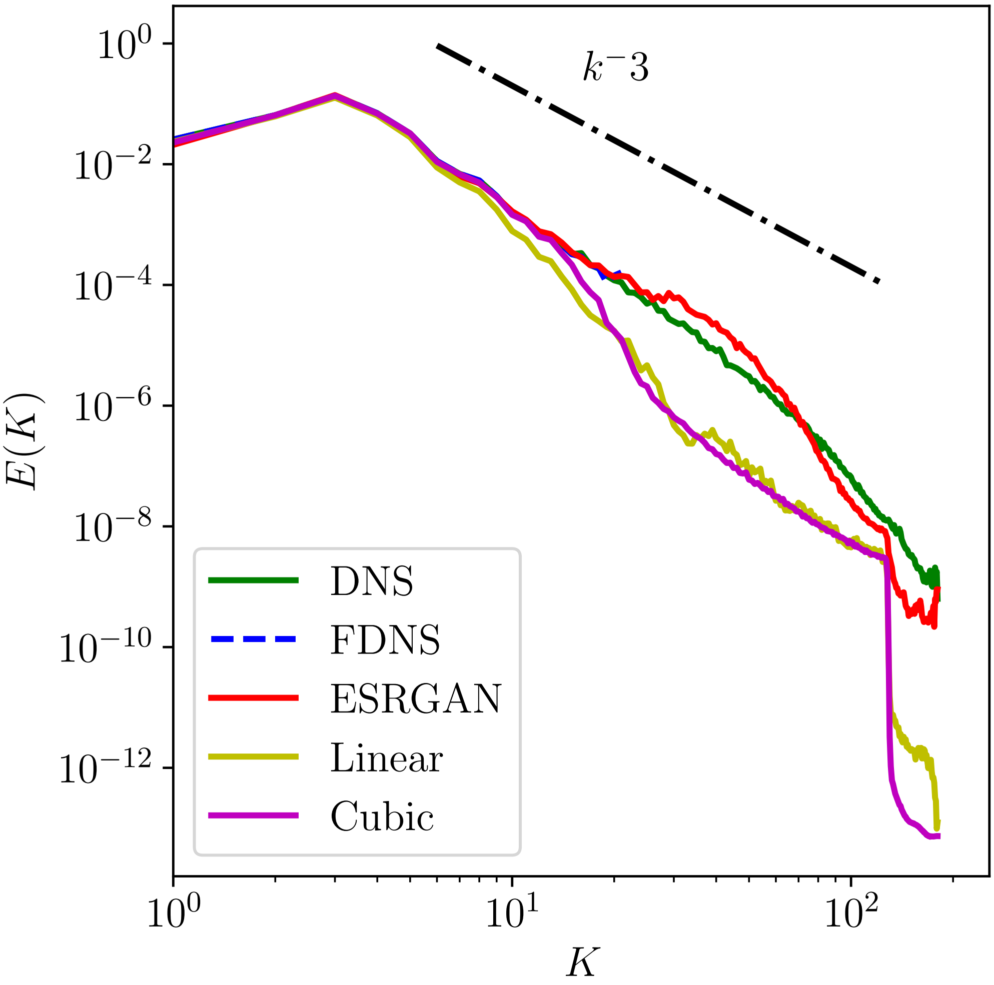

Figure 7: Energy Spectrum at time $t = 4.0$ s. FDNS refers to filleted DNS field.